frontiers | Frontiers in Marine Science

TYPE Original Research
PUBLISHED 11 October 2022
DOI 10.3389/fmars.2022.874759

OPEN ACCESS

EDITED BY
Dalton Hardisty,
Michigan State University,
United States

REVIEWED BY
Chelsie N. Bowman,
Georgia Southern University,
United States
Charles Diamond,
University of California, Riverside,
United States

*CORRESPONDENCE
Zunli Lu
zunlilu@syr.edu

SPECIALTY SECTION
This article was submitted to Marine Biogeochemistry, a section of the journal Frontiers in Marine Science

RECEIVED 12 February 2022
ACCEPTED 30 August 2022
PUBLISHED 11 October 2022

CITATION
He R, Elrick M, Day J, Lu W and Lu Z (2022) Devonian upper ocean redox trends across Laurussia: Testing potential influences of marine carbonate lithology on bulk rock I/Ca signals.
Front. Mar. Sci. 9:874759.
doi: 10.3389/fmars.2022.874759

Devonian upper ocean redox trends across Laurussia: Testing potential influences of marine carbonate lithology on bulk rock I/Ca signals

Ruliang He[1,2], Maya Elrick[3], James Day[4], Wanyi Lu[2] and Zunli Lu[2]*

[1]State Key Laboratory of Continental Dynamics, Shaanxi Key Laboratory of Early Life and Environments, Department of Geology, Northwest University, Xi'an, China, [2]Department of Earth and Environmental Sciences, Syracuse University, Syracuse, NY, United States, [3]Earth and Planetary Sciences, University of New Mexico, Albuquerque, NM, United States, [4]Department of Geography-Geology, Illinois State University, Normal, IL, United States

The Devonian is characterized by major changes in ocean-atmosphere O_2 concentrations, colonialization of continents by plants and animals, and widespread marine anoxic events associated with rapid $\delta^{13}C$ excursions and biotic crises. However, the long-term upper ocean redox trend for the Devonian is still not well understood. This study presents new I/Ca data from well-dated Lower Devonian through Upper Devonian limestone sections from the Great Basin (western Laurussia) and the Illinois Basin (central Laurussia). In addition, to better address potential influences of lithology and stratigraphy on I/Ca redox signals, I/Ca data are reported here as carbonate lithology-specific. Results indicate that lithologic changes do not exert a dominant control on bulk carbonate I/Ca trends, but the effects of some diagenetic overprints cannot be ruled out. For the Illinois Basin, low I/Ca values (more reducing) are recorded during the Pragian to Emsian and increased but fluctuating values are recorded during the Eifelian to Givetian. The Great Basin I/Ca trends suggest local upper oceans were more reducing in the Lochkovian, more oxic in the Pragian-Emsian, return to more reducing in the Eifelian, then to increasingly more oxic, but fluctuating in the Givetian-Frasnian. The local I/Ca variations at Great Basin likely share more similarity with global upper ocean condition (compared to the Illinois Basin) based on its position adjacent to the Panthalassic Ocean and its temporal co-variation with global environmental volatility trends. The overall reducing and variable redox conditions of local upper ocean (if not a diagenetic signal) during the Middle and Late Devonian of Great Basin coincide with evidence of increased global environmental volatility suggesting seawater redox may have been an important part of environmental instability at this time.

KEYWORDS

Devonian, Great Basin, Illinois Basin, I/Ca, seawater redox

1 Introduction

1.1 Devonian environmental changes and ocean redox conditions

The Earth system went through profound changes during the Devonian (419.2 to 358.9 Ma). Atmospheric pO_2 increased to near-modern levels, as suggested by multiple lines of geochemical (Dahl et al., 2010; Wallace et al., 2017; Lu et al., 2018; Elrick et al., 2022) and modeling evidence (Lenton et al., 2016; Krause et al., 2018). At the same time, vascular plants diversified (Gensel and Andrews, 1987; Elick et al., 1998; Meyer-Berthaud et al., 1999; Stein et al., 2007; Kenrick and Strullu-Derrien, 2014; Dahl and Arens, 2020) and may have driven increased pO_2 level by increasing organic carbon burial (Kump, 1988; Lenton et al., 2016). In the Mid-Late Devonian, the development in size and root depths of vascular plants are hypothesized to have enhanced continental weathering rates and nutrient load to oceans, resulting in episodes of elevated marine primary productivity, marine anoxia and widespread deposition of black shales (Algeo and Scheckler, 1998).

The significant increase in atmospheric and oceanic oxygen levels did not apparently result in long-term environmental stability. Instead, Brett et al. (2020) suggested that biologic and environmental responses show a range of volatility (e.g., fluctuations of surface seawater temperatures (SST), $\delta^{13}C$, eustasy, and hypoxic or anoxia-induced biotic turnovers/extinctions). For example, the Early Devonian is characterized by infrequent but large global carbon isotope fluctuations and fewer bio-crises (Brett et al., 2020) (e.g., Klonk event). In contrast, during the Middle and Late Devonian, frequent marine bio-crises occurred, such as the Hangenberg, Kellwasser, Taghanic, Kačak and Chotěc events, coinciding with the accumulation of widespread organic-rich marine facies and positive carbon isotope excursions (House, 2002; Becker et al., 2016; Becker et al., 2020).

Marine redox conditions may have played an important role. Lithological and geochemical evidence suggests that most of Late Devonian bio-events are associated with short-lived (Myr-scale) anoxic conditions in bottom waters (e.g., Murphy et al., 2000; Werne et al., 2002; Sageman et al., 2003; Rimmer, 2004; Lash and Blood, 2014; White et al., 2018). However, these intervals of black shale deposition and coeval bio-crises provide only brief snapshots of redox conditions for Late Devonian. The newly published U isotope data from marine limestones provides the first long-term redox constraint for the Devonian global ocean (Elrick et al., 2022). Additional local redox data, from the Devonian shallow oceans where most paleoenvironmental and paleontological signals are preserved, will be helpful for untangling the relationship among environmental volatility, changes in the biosphere, and ocean redox conditions during the Devonian.

In this study, we 1) evaluate upper ocean redox patterns from the interval spanning the Early to Late Devonian (Lochkovian-Frasnian) using carbonate lithology-specific I/Ca trends from the Great Basin and Illinois Basin, 2) compare these results to existing I/Ca trends from the Middle Devonian of the Appalachian Basin, and 3) discuss the combined Laurussia-wide upper ocean redox trends with previously identified global paleoenvironmental volatility patterns (Brett et al., 2020).

1.2 Carbonate lithology-specific approach

As marine carbonate rocks usually have heterogenous compositions with various biogenic and non-biogenic components precipitated in different water depths, including porewater, I/Ca records measured from bulk carbonate rocks may represent a mixed signal. For example, I/Ca signals can vary among different foraminifera species and associated coarse bulk fraction within the same Cenozoic core (e.g., Zhou et al., 2014; Zhou et al., 2016). Indeed, the influence from lithologic changes is an unavoidable issue for all bulk carbonate geochemical proxies, especially for long-term reconstructions that contain different depositional facies, including I/Ca used here. For research focusing on deep-time samples, it is challenging to generate long-term, continuous I/Ca profiles for a specific carbonate component. In this study, we attempt a new approach, namely a carbonate lithology-specific I/Ca investigation, on Devonian limestones from the Great Basin and Illinois Basin, by identifying facies for each sample and assessing influences they might have on I/Ca values.

1.3 Iodine as a redox proxy

Iodine is an important element for biogeochemical and redox reactions (Küpper et al., 2011). In the modern seawater, iodine has a residence time of ~ 300 kyr and a uniform concentration of ~ 0.45 μmol/L (Elderfield and Truesdale, 1980) and its concentration can be an order of magnitude lower in freshwater (Fehn, 2012). For two thermodynamically stable iodine species, iodate (IO_3^-) is the major species in well-oxygenated waters (Truesdale and Bailey, 2000), while iodide (I^-) dominates at depth in anoxic waters (Wong and Brewer, 1977) and in anoxic porewaters (Kennedy and Elderfield, 1987a, b).

Iodate is the only species that can be incorporated into the carbonate crystal lattice (Lu et al., 2010) by substituting of CO_3^{2-} with IO_3^- (Podder et al., 2017; Feng and Redfern, 2018). Therefore, high I/Ca ratios found in bulk carbonate rocks indicate precipitation from more oxic upper ocean waters where iodate is present, although the oxidation rate can be very slow (Hardisty et al., 2020). Low I/Ca values may represent

the development of O_2-depleted conditions in or near the upper ocean or the influence from diagenetic process which is only known to reduce original values (Hardisty et al., 2017). The proxy has been widely applied to bulk carbonate samples to study the relationships among local ocean redox changes, major climate changes, and bio-crises from the Proterozoic and Phanerozoic (e.g., Zhou et al., 2015; Lu et al., 2017; Liu et al., 2019; Shang et al., 2019; He et al., 2020a; He et al., 2020b). More details about the I/Ca proxy are discussed in the recent review by Lu et al. (2020b).

2 Geological background

The Devonian Great Basin succession in Nevada accumulated in the southern subtropics along the westward-deepening epicontinental seaway of western Laurussia (Morrow and Sandberg, 2008) (Figures 1, S1). The western margin of Laurussia accumulated passive-margin deposits from the late Proterozoic through Middle Devonian followed by foreland basin deposits (associated with the Antler orogeny) in the Late Devonian through Early Mississippian (Morrow and Sandberg, 2008). The Great Basin composite section (~800 m) spans the middle Early Devonian through early Late Devonian (middle Lochkovian to middle Frasnian). Two central Nevada locations were sampled, including Coal Canyon (Simpson Park Range) and the northern Antelope Range (Figure S1). For each section, we used previously reported conodont biostratigraphy to determine zone-level age control and to correlate sections (section 1 in supplementary discussion). The Coal Canyon (Lochkovian) section represents deposition seaward of the shelf edge in basinal environments (Johnson and Murphy, 1984). The northern Antelope section (Pragian to Frasnian) represents basinal, slope, shelf edge, and middle shelf environments depending on the position of eustatic sea level (Johnson et al., 1996; Morrow and Sandberg, 2008). Parts of the Emsian, Givetian, and Frasnian were deposited in basinal environments in the northern Antelopes.

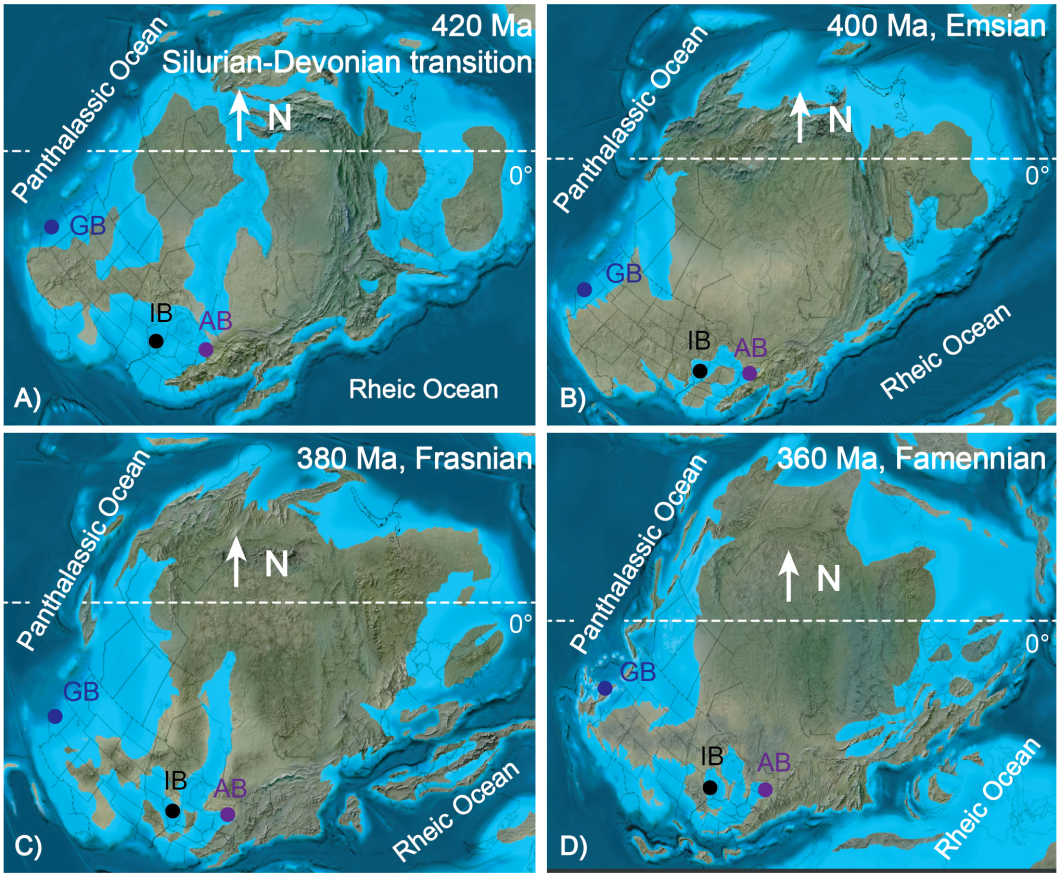

FIGURE 1
Paleogeographic maps of Laurussia during different stages **(A–D)** of Devonian. Maps are based on Blakey (2018). Dashed white lines represent the paleo-equator. GB represents the location of Great Basin composite section. IB represents the location of Illinois State Geological Survey White County Core of Illinois Basin. AB represents the location of the Middle Devonian core from the Appalachian Basin (He et al., 2020b).

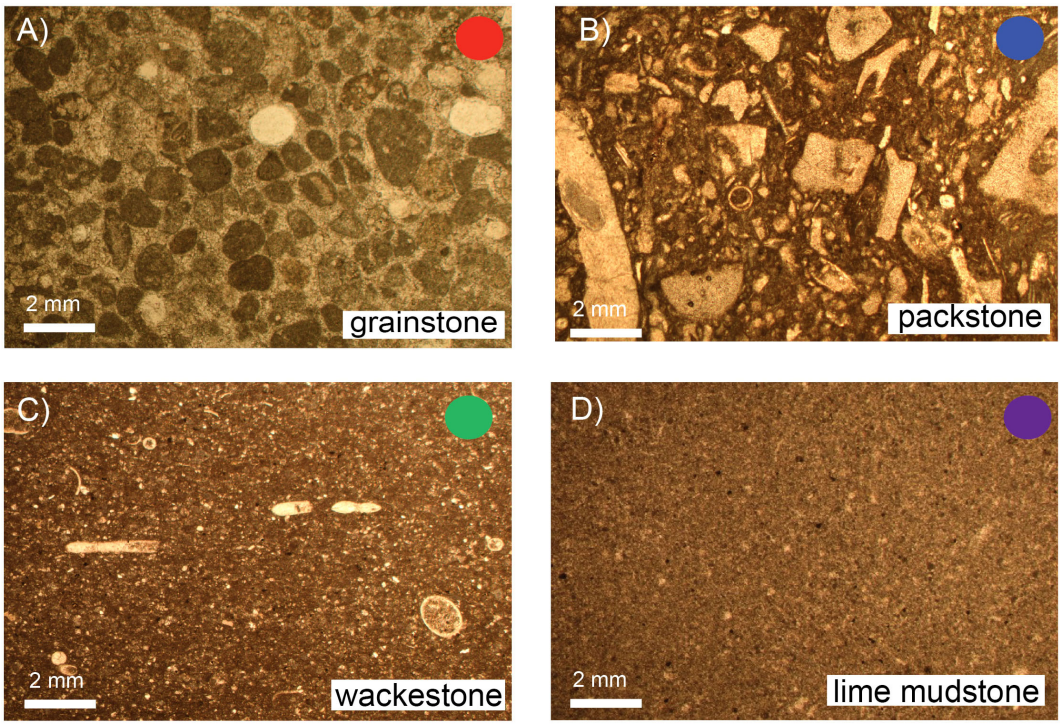

FIGURE 2
Thin section photographs of the main four lithologic groups identified in the composite Great Basin section of Nevada. Photos were taken under plane-polarized light. The colored solid circles are consistent with the colors shown in Figures 3–6 and S2. From **(A–D)**, lithologic transitions are from coarse grained to fine grained and depositional environments transition from upper shoreface to offshore environments. Note abundant early marine cements in the grainstone of **(A)**.

The Illinois Basin is one of the major interior cratonic basins of Laurussia, and accumulated up to 4.5 km of Cambrian through Pennsylvanian marine carbonate and siliciclastic deposits (Buschbach and Kolata, 1990; Kolata and Nelson, 1990). I/Ca data of Illinois Basin are measured from samples of the Illinois Geological Survey White County Core (~110 m thick; Figure 1) that spans the Pragian to early Givetian. The succession accumulated in shallow-water epicontinental sea carbonate settings in the southern subtropics of central Laurussia (Figure 1). The connection to the adjacent Rheic Ocean was restricted during Early Devonian eustatic lowstands, but became more open as eustatic sea level rose in the Middle and Late Devonian (Johnson et al., 1985) (Figure 1). Relative age control comes from conodont biostratigraphy (Day et al., 2012).

3 Samples and methods

3.1 Sample preparation

Samples for I/Ca and trace element analysis for the Great Basin section were collected at ~5-10 m intervals and at ~1-5 m intervals for C isotopes. To establish a carbonate lithology-specific I/Ca profile, the sections were described on a bed-by-bed basis using traditional field- and petrographic-based observations of grain size, sedimentary structures, color, fossil types/abundance, and facies associations. For the Illinois Basin core, samples were collected at ~1-3 m intervals for I/Ca analysis and carbonate lithologies were interpreted from core observations. Samples for elemental analyses were collected at ~5-10 m intervals for Great Basin and ~1 m intervals for Illinois Basin, and were chipped into small, non-weathered fragments, and were powdered in a Spex shatterbox with an alumina puck pulverizer. It should be noted that all the powdered samples are from rock fragments, rather than from micro-drilled carbonate powders.

3.2 I/Ca measurements

A total of 129 samples for Great Basin section and 77 samples for Illinois Basin core were selected for iodine analysis. Around 2-5 mg powdered samples were weighed and then rinsed with deionized (DI) water to remove any iodine that is attached on the surface of sample. To extract iodine from the

carbonate fraction, diluted HNO_3 (3% by volume) was added to clean powders in microcentrifuge tubes and the solution was separated from the residuals immediately after samples stopped reacting. The dissolved fraction was then diluted to solutions of ~ 50 ppm Ca and mixed with a matrix solution containing internal standards (Cs and In) and buffered with tertiary amine. Measurements of iodine, calcium and magnesium concentrations were performed on a quadrupole inductively coupled plasma mass spectrometer (ICP-MS, Bruker M90) at Syracuse University. The precisions are typically better than 1% for ^{127}I and the detection limit is usually better than 0.1 μmol/mol. The long-term accuracy is guaranteed by frequently repeated measurements of the standard reference material JCp-1 (Lu et al., 2020b).

3.3 C isotope, major and trace elements measurements

Carbonate C isotope measurements were performed at the University of New Mexico Center for Stable Isotopes. Isotope values were analyzed using continuous flow Isotope Ratio Mass Spectrometry with a Gasbench device coupled to a Thermo Fisher Scientific Delta V Plus Isotope Mass Spectrometer. The reproducibility was better than 0.1‰ for $\delta^{13}C$ based on repeats of laboratory standard (Carrara Marble) and the laboratory standards were calibrated versus NBS 19.

For elemental analyses, rock powders were dissolved in 1 M HNO_3, and solutions were centrifuged to remove insoluble residue. A solution split was diluted to ~200 ppm Ca with 2% HNO_3 and analyzed for a full suite of major, trace, and rare-earth element abundances on a Thermo Scientific ICAP-Q inductively coupled plasma mass spectrometer (ICP-MS) at Arizona State University. The analytical precision for all elements of interest was <5%.

4 Results

4.1 Great Basin

The I/Ca trends are divided into four stratigraphic intervals (Figures 3, 5). The Lochkovian consistently records low I/Ca with most of values lower than 1 μmol/mol, followed by an abrupt increase to 1 to 3 μmol/mol during the Pragian and Emsian. Near the Emsian-Eifelian unconformable boundary, I/Ca shifts back to nearly 0 μmol/mol and remains near detection limit through the Eifelian, except for a short-term I/Ca excursion of up to ~ 1.5

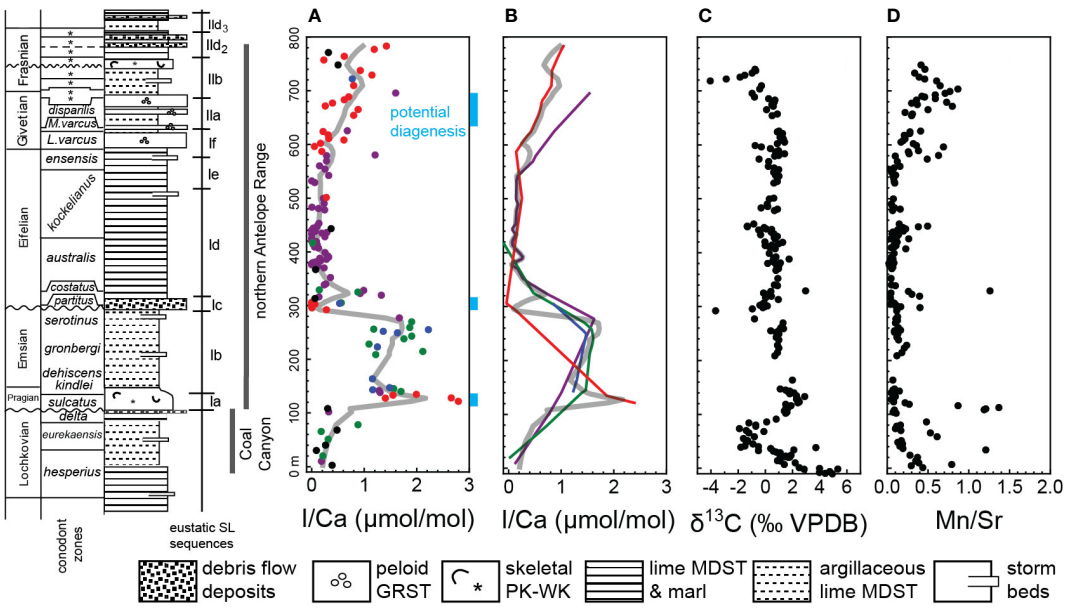

FIGURE 3
Geochemical measurements of the Great Basin composite section: **(A)** carbonate lithology-specific I/Ca ratio, **(B)** LOWESS smoothing trends for four lithologic facies, **(C)** bulk carbonate carbon isotopes, **(D)** Mn/Sr ratios. Color code for lithological groups: grainstone (red), packstone (blue), wackestone (green), lime mudstone (purple), unassigned (black). The thicker gray lines in **(A, B)** show the LOWESS smoothing results of all the samples, while other colored lines represent the LOWESS smoothing for each lithological group (with the same color code as the dots). GRST, grainstone; PK, packstone, WK, wackestone; MDST, mudstone, SL, sea level. Blue lines in **(A)** represent intervals that may record potential diagenetic alteration. *Conodont zones not labelled are (in ascending order): *norrisi, MN 1-2, MN 3, MN 6, hassi-jamieae, l. rhenana, u. rhenana, linguiformis*.

μmol/mol. From the Givetian to Frasnian, I/Ca gradually increases to ~ 2 μmol/mol, but shifts back to near zero values episodically and fluctuates in the range of 0 to 2 μmol/mol. Nevertheless, the overall I/Ca average of Givetian-Frasnian interval is lower than that of the Pragian-Emsian (Figure 5).

4.2 Illinois Basin

I/Ca values are consistently low (< 0.5 μmol/mol) in the Pragian and Emsian (Figure 4A). In the early Eifelian, values increase slightly to ~0.5 μmol/mol until the late Eifelian with a brief peak to ~1 μmol/mol, followed by an increase to fluctuating values (up to ~ 3 μmol/mol) in the late Eifelian through Givetian (Figure 4A). The timing of the major I/Ca increase and fluctuating values during the Givetian is coeval to that observed in the Great Basin section (Figure 3A).

5 Discussion

5.1 Carbonate lithology-specific I/Ca record

Geochemical measurements conducted on bulk carbonate rock samples are potentially influenced by lithologic variability and diagenesis. To avoid effects of lithologic influences, measurements can be performed on specific biologic components, such as individual brachiopod calcite or conodont apatite (van Geldern et al., 2006; Joachimski et al., 2009), but then the sample resolution is limited by available facies containing appropriate fossil types and abundances. On the other hand, some studies compare stratigraphic trends of redox proxies to sedimentologic and petrographic characteristics and fossil assemblages to investigate the nature of geochemical signals (e.g., Bowman et al., 2020). We take a similar approach for this study and compare I/Ca values and trends to specific carbonate rock types and sequence stratigraphy (Figures 3, 4).

For the Great Basin, the sampled carbonate rocks span the entire scheme of Dunham's classification, from grainstone to lime mudstone (Dunham, 1962). Using field and petrographic observations, the stratigraphy was subdivided into four major depositional groups including: upper shoreface (composed of skeletal/peloid grainstones-packstones), lower shoreface (skeletal packstones-wackestones), and moderately to poorly oxygenated offshore (bioturbated skeletal lime mudstones-wackestones and lime mudstones) (Figure 2). The lime mudstone that represents a low-energy environment is a dominant part of the Eifelian (~ 300 - 600 m; Figure 3). Tentaculinids are found in mudstones of the lower *australis* zone of the Eifelian (325 - 370 m). Skeletal wackestone and

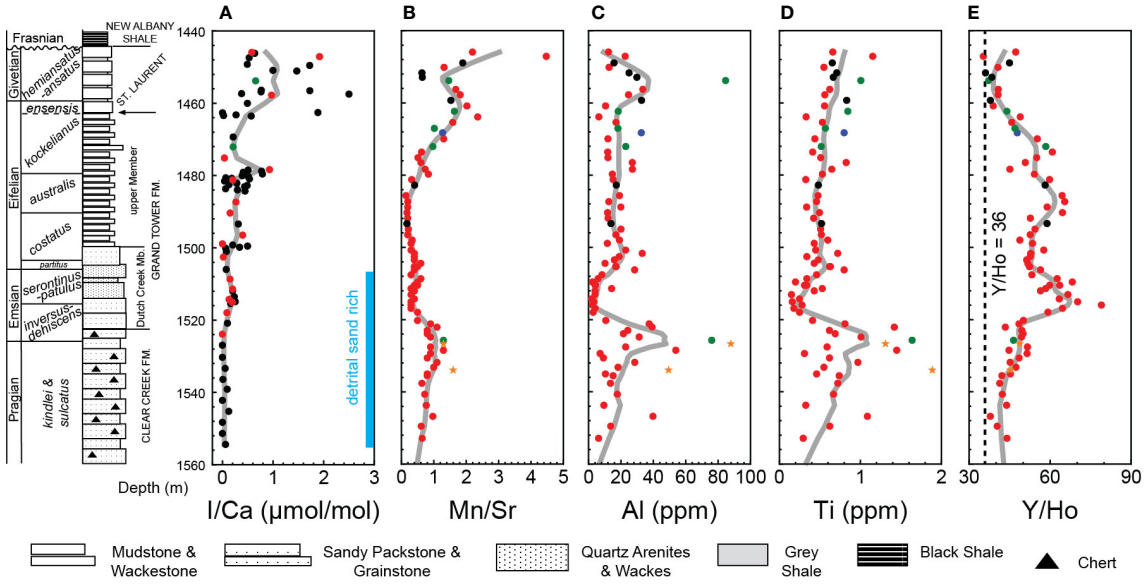

FIGURE 4
Geochemical measurements from the Illinois Basin core. **(A)** Carbonate lithology-specific I/Ca ratios, **(B)** Mn/Sr ratios, **(C)** Al concentration, **(D)** Ti concentration, **(E)** Y/Ho ratios. The gray curves show the results of LOWESS smoothing. The black dashed line in **(E)** shows Y/Ho = 36. Values higher than 36 indicate primary marine REEs signals [e.g., Ling et al. (2013)]. Note all the results were measured from the carbonate fraction. The Pragian-Emsian portion is rich in quartz sands (blue vertical line). Samples of **(A)** and samples of **(B–E)** are from the same core but not measured from same depth. Color code for lithological groups: grainstone (red), packstone (blue), wackestone (green), lime mudstone (purple), unassigned (black). Brown stars in Pragian of **(B–E)** represent quartz sandstones with calcite cements.

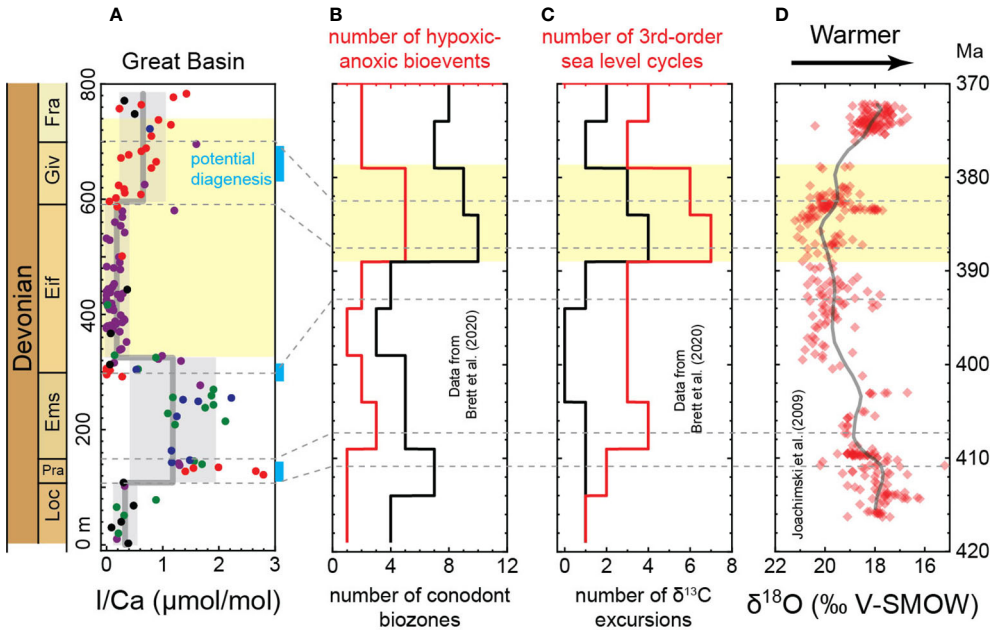

FIGURE 5
I/Ca ratios of the Great Basin section and compiled Devonian environmental and biotic parameters. **(A)** Stratigraphic trends of I/Ca are subdivided into four intervals; the straight gray lines represent averages of I/Ca within each interval, and the gray boxes show the ranges of one standard deviation. **(B, C)** Numbers of conodont biozones, hypoxic/anoxic-related bioevents, carbon isotope excursions, global sea level changes within Devonian time bins of 5 Myr durations. Data are modified from Tables 2 and 4 of Brett et al. (2020) and we used the subdivided zonation for conodont zones here. **(D)** Global records of oxygen isotopes of conodont apatite (Joachimski et al., 2009). The gray curve in **(D)** represents locfit regression of Joachimski et al. (2009). The gray dashed lines correlate the Great Basin stage boundaries to those of the compiled datasets. The yellow boxes highlight the intervals of highest volatility identified by Brett et al. (2020). Color code for lithological groups: grainstone (red), packstone (blue), wackestone (green), lime mudstone (purple), unassigned (black).

packstone compose most of the Lower Devonian (Figure 3). Skeletal grainstones are observed in the Pragian and the grainstones with crinoid can be found in the bottom of the Eifelian. Last, the Givetian and Frasnian contain abundant peloid grainstones. Therefore, the four facies are unevenly distributed throughout the composite section (Figure 3). The stratigraphic I/Ca trends of each facies are plotted individually (Figure 3B) to investigate the influence of carbonate facies on I/Ca values. We found I/Ca ratios of each facies consistently show similar stratigraphic trends as the overall trend that combines all the facies, except the succession of Emsian grainstones due to the absence of samples (Figures 3A, B). Moreover, all four facies have a wide range of I/Ca values (Figure 3). For example, relatively low Lochkovian and Eifelian I/Ca values occur in all four facies and the same is true of the higher I/Ca values that occur in the Emsian, late Givetian and early Frasnian (Figure 3B). In addition, I/Ca trends show no systematic variations across eustatically generated, Myr-scale, sequence boundaries, except for relatively abrupt I/Ca changes near the two Lower Devonian unconformities (Figure 3). Therefore, the lithological variation across the composite section does not have a major influence on stratigraphic I/Ca trends.

The majority of the Illinois Basin samples are composed of shallow-water crinoidal grainstones with minor calcite-cemented quartz sandstone in the Pragian and skeletal wackestone and packstone in the upper Eifelian to Givetian. The predominance of grainstone limits robust evaluation of relationships between the full range carbonate facies types and I/Ca values (Figure 4A). The Pragian to Emsian grainstones contain abundant quartz sands and the rock type records lower I/Ca ratios (Figure 4). The detrital quartz component is likely related to fluvial input during long-term eustatic sea level lowstand. The influx of fluvial waters with lower iodine concentrations may explain the lower I/Ca values in this interval.

This approach of reporting detailed carbonate lithology along with bulk rock I/Ca measurements may have important potential in assisting the interpretations of bulk carbonate I/Ca analyses. It is a logic similar to utilizing species-specific foraminiferal records during the Cenozoic (e.g., Zachos et al., 2001). We suggest this approach be adopted in future deep-time I/Ca carbonate studies.

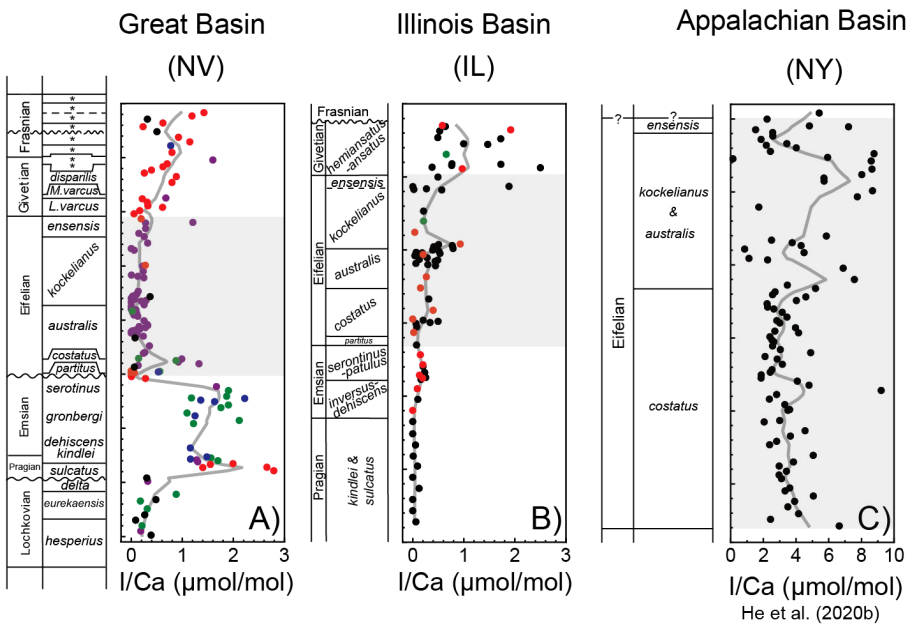

FIGURE 6
I/Ca comparisons among the three basins: **(A)** Great Basin, **(B)** Illinois Basin, **(C)** Appalachian Basin (He et al., 2020b). Gray shadings identify the Eifelian interval overlapping between all three basins for comparison. A closer comparison for the Eifelian stage is in Supplementary Figure S2. Color code for lithological groups: grainstone (red), packstone (blue), wackestone (green), lime mudstone (purple), unassigned (black). *Conodont zones not labelled are (in ascending order): *norrisi, MN 1-2, MN 3, MN 6, hassi-jamieae, l. rhenana, u. rhenana, linguiformis*.

5.2 Diagenetic influences

A detailed study of Neogene-Quaternary Bahamian carbonates evaluated I/Ca values of diagenetically altered samples and documented that diagenesis (including dolomitization) reduced rather than increased original I/Ca values in all cases (Hardisty et al., 2017).

In the Great Basin, thin section observation indicates that grainstones contain abundant early marine cements, especially in the Pragian, Eifelian, Givetian, and Frasnian (labeled in Figure 3A). Thus, it suggests the grainstones may have experienced some level of diagenetic iodate loss. Therefore, the occurrence of grainstones throughout the Great Basin section and the potential for diagenetic iodate loss may explain some of the observed I/Ca trends. For example, fluctuating Givetian-Frasnian I/Ca values may represent the effects of intermittent diagenetic iodate loss rather than original fluctuating redox conditions (Figure 3A). Mn/Sr values also aid in evaluating the effects of diagenesis. Due to the difference in mobility of Sr and Mn, higher Mn/Sr ratios are usually generated after stronger rock-fluid reactions with reducing fluids and can be used to evaluate the overprint from diagenesis (Lohmann, 1988). Relatively low Mn/Sr (<2) ratios throughout the section suggest the interaction with Mn-rich anoxic porewater was limited. Low Mg/Ca ratios (with most ratios <0.1 mol/mol) suggest dolomitization was minor (Supplementary Table 1).

In the Illinois Basin, limestone samples of Pragian to Emsian contain abundant detrital quartz sands with calcite cements (Figure 4). This calls into question the primary nature of the I/Ca signal in this interval and the influences due to diagenesis. Future work that details the I/Ca values from specific components of heterogenous limestones or additional samples from better preserved sections are required to interpret whether the observed signal records primary or altered redox trends. Mn/Sr values are lower than 2 for most of the samples, except for the uppermost Eifelian to lower Givetian where Mn/Sr values reach up to 4.5 (Figure 4B). If this part of the section with higher Mn/Sr values reflects a more diagenetically altered interval, original I/Ca ratios could have been higher due to diagenetic iodate loss (Figure 4). Last, the overall low Mg/Ca (most ratios < 0.1 mol/mol) also suggests limited dolomitization (Supplementary Table 3).

5.3 Local redox conditions of Great Basin and Illinois Basin

5.3.1 Great Basin

Although some grainstone samples of the Great Basin section may have been influenced by the diagenetic iodine loss (Figure 3A), I/Ca values of grainstones are not consistently low (especially the Pragian and Frasnian) and they still follow the stratigraphic trend of other facies (Figure 3B), suggesting

diagenesis may not totally erase the original signals. Therefore, combining with data from other facies, it is possible that our I/Ca data captures general trends in local primary seawater redox. If correct, relatively higher I/Ca values of the Pragian-Emsian suggest the local seawater may have been more oxic during Early Devonian, except the Lochkovian. On the other hand, a relatively lower I/Ca background during the Eifelian may be related to more anoxic conditions; in addition, more oxic conditions may have developed locally in the Givetian and Frasnian, indicated by higher I/Ca values. It should be noted that the low I/Ca values may reflect carbonate precipitation from waters close to the OMZ or oxycline, rather than directly within anoxic waters, because recent studies suggested that the I/Ca sometimes is more related to a mixing of regional marine redox environments rather than *in situ* processes (Lu et al., 2020a; Hardisty et al., 2021).

5.3.2 Illinois Basin

Illinois I/Ca trends do not match the Great Basin, especially during the Pragian-Emsian, with consistently low I/Ca ratios close to 0 μmol/mol (Figure 4A). If diagenesis did not uniformly reset I/Ca ratios of these samples to nearly 0 μmol/mol during the Eifelian, the relatively low I/Ca background of the Eifelian is consistent with the anoxic conditions recorded in the Great Basin. From the late Eifelian to early Givetian, the overall increased I/Ca values indicate increased local oxygenation (Figure 4A). The fluctuating I/Ca signal during this interval may be related to a frequently shifting redox conditions or simply reflect diagenetic iodate loss considering the higher Mn/Sr ratios found at this interval (Figure 4).

5.4 Inter-basinal comparison: influence of paleogeography

Paleogeography can influence I/Ca as a local redox proxy, since iodine chemistry in the water column can be influenced by local hydrography, local redox, and also major changes in global ocean conditions (e.g., Zhou et al., 2015). Based on the paleogeographic reconstructions (Figure 1 and Morrow and Sandberg, 2008), the Great Basin section was located along the western margin of Laurussia and connected directly to the Panthalassic Ocean during the Devonian. Development of an OMZ is very common in western continental margins in the tropics and subtropics (Hay, 1995), such as the modern eastern tropical Pacific where the upwelling-driven productivity and poor ventilation result in a large OMZ. Although the Devonian Great Basin was a shallow epeiric sea, its redox condition can still be influenced by OMZ that may have developed along the west margin of Laurussia. In contrast, the Illinois and Appalachian basins were isolated epeiric sea basins situated in central and eastern margin of Laurussia continent at higher latitudes (~ 30°S; Figure 1). The I/Ca range found in the Great Basin is lower than that of the Appalachian Basin (e.g., during the Eifelian; Figures 6 and S2). During the Late Ordovician, a western Laurentia continental margin site closer to the upwelling and OMZ also had a relatively lower range of I/Ca than the section from eastern Laurentia (Pohl et al., 2021), suggesting similar paleogeographical redox patterns.

The different stratigraphic I/Ca trends and ranges in Appalachian and Illinois Basins may also be related to the variable restriction to the Panthalassic Ocean. The paleoceanographic conditions of Devonian epeiric seas (i.e., Illinois and Appalachian basins) are not well-constrained. The difference between the Eifelian I/Ca trends in the Illinois Basin and Appalachian Basin is likely due to the >1500 km distance between the locations, physical separation by exposed arches and sills during lower eustatic sea levels of the Early-Middle Devonian. This interpretation of lateral redox and salinity changes in the Middle Devonian epeiric seaway is consistent with the super-estuarine circulation model in which the lateral advection of deeper water from open ocean controls the redox condition of epeiric seas (Algeo et al., 2008) and spatially heterogenous Fe speciation and trace metals within Late Devonian Appalachian Basin (Gilleaudeau et al., 2021). The uniformly low I/Ca background (nearly 0 μmol/mol) of Pragian-Emsian Illinois Basin strata may also be related to mixing with fresh water from fluvial discharge during lower eustatic sea levels. Although the modern seawater-like Y/Ho ratios (>36) suggest a deposition in a marine environment, terrestrial sand content and elevated Al and Ti concentration indicate the contribution from terrestrial processes cannot be excluded (Figure 4 and the section 2 of Supplementary Discussion).

5.5 Devonian seawater redox conditions

Both proxy (Mo isotope, U isotope, I/Ca ratio, Ce anomaly and charcoal abundance) and model (COPSE and GEOCARBSULF) results suggest atmospheric pO_2 levels increased during the Devonian (Dahl et al., 2010; Glasspool and Scott, 2010; Lenton et al., 2016; Wallace et al., 2017; Krause et al., 2018; Lu et al., 2018; Elrick et al., 2022). The increase in I/Ca ratios from Lochkovian to Emsian in the Great Basin section (Figure 3A) could be related to the rise of atmospheric oxygen levels impacting the upper ocean. Since I/Ca itself is a local marine redox proxy and not a direct proxy for atmospheric oxygen levels, I/Ca data from multiple locations in addition to Laurussia or additional evidence from independent global redox proxies will be required to pin down the timing of Devonian pO_2 rise.

5.6 Devonian environmental volatility

As the publications of high-resolution radiometric ages for the Devonian accumulate, Brett et al. (2020) are able to

investigate the environmental volatility based on the frequency of fluctuations in environmental and biotic parameters, including SST, $\delta^{13}C$, eustasy, and hypoxic or anoxia-induced biotic turnovers/extinctions (Figure 5). A higher environmental volatility is usually considered as more frequent occurrences of environmental and biotic events over a given interval of time (e.g., number of events per million years). Brett et al. (2020) suggests a relatively less volatile interval from the Lochkovian to middle Eifelian, followed by peak environmental volatility during the late Eifelian through early Frasnian with more frequent occurrences of biozone turnover, hypoxic-anoxic events, C isotope excursions and sea level changes (Figures 5B, C). The mechanism behind the increased environmental volatility is not well understood; however, this time interval coincides with lower SST (Joachimski et al., 2009), orbital-scale glacio-eustasy (Elrick and Witzke, 2016), more frequent Myr-scale sea-level changes, and increased continental weathering (van Geldern et al., 2006) (Figure 5).

Here, we compare the Devonian environmental volatility with I/Ca ratios from Great Basin under the assumption that it may record the most primary seawater redox trends. The more oxygenated upper ocean conditions during the Pragian-Emsian of the Great Basin, suggested by the higher I/Ca ratios, are consistent with the notion of relatively stable Early Devonian biotic environments (Figure 5). The onset of high-volatility environments starts at the late Eifelian (Brett et al., 2020). Due to an unconformity along the Emsian-Eifelian boundary (missing *partitus* and parts of *serotinus* and *patulus* zones) and low sedimentation rates (especially for the *costatus* zone), the lower Eifelian is very thin in the Great Basin section (Figure 3). Therefore, the boundary between the *costatus* and *australis* zones of upper Eifelian at ~ 325 m is equivalent to the onset of high volatility (Figures 3, 5). I/Ca trends in the Great Basin suggest an expansion of OMZ from the early into the late Eifelian, followed by OMZ fluctuations during Givetian-Frasnian, so the I/Ca data largely echoes the reconstructed environmental volatility (though not strictly with a one-to-one match). Even though I/Ca data from a single location records local redox conditions, the redox changes can still mimic the global ocean redox evolution (Lu et al., 2020b). It is not unreasonable to suggest that the local Great Basin water column captured some fundamental changes in global redox trends, considering the coincidence between I/Ca ratios and environmental volatility and the proximity and connectedness to the Panthalassic Ocean.

Previous studies interpret that many Devonian bio-events, for example Taghanic, Kellwasser, Hangenberg and other less significant events that are classified by Becker et al. (2016) as extinctions at lower taxonomic level (such as genera and species) with fewer groups, were the result of expanded anoxia (e.g., Zambito et al., 2012; Formolo et al., 2014; White et al., 2018; Liu et al., 2019; Zhang et al., 2020). In this study, although the frequent occurrences of biozone turnovers and bio-events in the late Eifelian to early Frasnian correlate with overall more reducing conditions in the Great Basin, we do not find a one-for-one co-variation between upper ocean redox conditions in our Great Basin section and those less significant bio-events. It indicates that ocean deoxygenation may not be the sole trigger for all the later Devonian bio-events.

6 Conclusion

Carbonate lithology-specific I/Ca data from Early to Late Devonian (Lochkovian to Frasnian) limestones accumulating in the Great Basin and Illinois Basin of Laurussia indicates that the overall I/Ca trends are not systematically influenced by lithology or eustatic sea-level changes. Upper ocean redox trends in the Great Basin are characterized by higher I/Ca values (more oxic conditions) in the Pragian-Emsian, a shift to lower values (more reducing conditions) in the Eifelian, followed by slightly higher and fluctuating I/Ca trends in the Givetian and Frasnian. The more reducing and fluctuating redox conditions in the Middle and Late Devonian are coincident with previously interpreted intervals of high environmental volatility. Illinois Basin I/Ca trends record low values (reducing conditions) in the Pragian-Emsian followed by increasing and fluctuating values in the Eifelian-Givetian. The different I/Ca signals between the two basins are likely related to variations in local upper ocean redox, hydrographic conditions associated with varying paleogeography and eustasy, and/or diagenesis. To further evaluate global versus local redox evolution of Devonian oceans, other I/Ca records and independent redox proxies from other locations are required along with additional indicators of diagenesis.

Data availability statement

The original contributions presented in the study are included in the article/Supplementary Material. Further inquiries can be directed to the corresponding author.

Author contributions

RH and ZL designed the study. RH wrote the draft with input from all coauthors. RH and WL carried out the I/Ca analyses. ME and JD collected samples. ME carried out lithologic analyses. All authors contributed to the article and approved the submitted version.

Funding

Partial funding for this study was provided by the National Science Foundation (OCE-1232620 and EAR-2121445 to ZL; EAR-1733991 to ME).

Acknowledgments

We would like to thank Charles Diamond, a reviewer, the guest editor Dalton Hardisty and two reviewers of an earlier submission for their constructive comments and suggestions. RH thanks the support from the Research Excellence Doctoral Funding (REDF) Fellowships of Syracuse University.

Conflict of interest

The authors declare that the research was conducted in the absence of any commercial or financial relationships that could be construed as a potential conflict of interest.

Publisher's note

Supplementary material

The Supplementary Material for this article can be found online at: https://www.frontiersin.org/articles/10.3389/fmars.2022.874759/full#supplementary-material

References

Algeo, T. J., Heckel, P. H., Maynard, J. B., Blakey, R., Rowe, H., Pratt, B., et al. (2008). "Modern and ancient epeiric seas and the super-estuarine circulation model of marine anoxia," in *Dynamics of epeiric seas: sedimentological, paleontological and geochemical perspectives*, vol. 48. (St. John's, Canada: Geological Association of Canada, Special Publication), 7–38.

Algeo, T. J., and Scheckler, S. E. (1998). Terrestrial-marine teleconnections in the Devonian: links between the evolution of land plants, weathering processes, and marine anoxic events. *Philos. Trans. R. Soc. London. Ser. B.: Biol. Sci.* 353, 113–130. doi: 10.1098/rstb.1998.0195

Becker, R. T., Königshof, P., and Brett, C. E. (2016). Devonian Climate, sea level and evolutionary events: an introduction. *Geologic. Soc. London. Special. Publications.* 423, 1–10. doi: 10.1144/SP423.15

Becker, R. T., Marshall, J. E. A., Da Silva, A. C., Agterberg, F. P., Gradstein, F. M., and Ogg, J. G. (2020). The Devonian period. *Geologic. Time. Scale.*, 733–810. doi: 10.1016/B978-0-12-824360-2.00022-X

Blakey, R. (2018) *Paleogeography and geologic evolution of north America*. Available at: https://deeptimemaps.com/ (Accessed March 2018).

Bowman, C. N., Lindskog, A., Kozik, N. P., Richbourg, C. G., Owens, J. D., and Young, S. A. (2020). Integrated sedimentary, biotic, and paleoredox dynamics from multiple localities in southern laurentia during the late Silurian (Ludfordian) extinction event. *Palaeogeogr. Palaeoclimatol. Palaeoecol.* 553, 109799. doi: 10.1016/j.palaeo.2020.109799

Brett, C. E., Zambito, J. J., McLaughlin, P. I., and Emsbo, P. (2020). Revised perspectives on Devonian biozonation and environmental volatility in the wake of recent time-scale revisions. *Palaeogeogr. Palaeoclimatol. Palaeoecol.* 549, 733–810. doi: 10.1016/j.palaeo.2018.06.037

Buschbach, T. C., and Kolata, D. R. (1990). *Regional setting of Illinois basin: chapter 1: part i. Illinois basin: regional setting*. AAPG MEMOIR.

Dahl, T. W., and Arens, S. K. M. (2020). The impacts of land plant evolution on earth's climate and oxygenation state – an interdisciplinary review. *Chem. Geology.* 547, 119665. doi: 10.1016/j.chemgeo.2020.119665

Dahl, T. W., Hammarlund, E. U., Anbar, A. D., Bond, D. P., Gill, B. C., Gordon, G. W., et al. (2010). Devonian Rise in atmospheric oxygen correlated to the radiations of terrestrial plants and large predatory fish. *Proc. Natl. Acad. Sci.* 107, 17911–17915. doi: 10.1073/pnas.1011287107

Day, J. E., Gouwy, S., and MacLeod, K. G. (2012). *Lower-middle Devonian (Pragian-lower givetian) conodont biostratigraphy, middle Devonian sea level record and estimated conodont apatite $\delta^{18}O$ sea surface temperature changes in the southern Illinois basin, USA*. GSA Annual Meeting, Charlotte, North Carolina, USA

Dunham, R. J. (1962). *Classification of carbonate rocks according to depositional textures.*

Elderfield, H., and Truesdale, V. W. (1980). On the biophilic nature of iodine in seawater. *Earth Planetary. Sci. Lett.* 50, 105–114. doi: 10.1016/0012-821X(80)90122-3

Elick, J. M., Driese, S. G., and Mora, C. I. (1998). Very large plant and root traces from the early to middle Devonian: Implications for early terrestrial ecosystems and atmospheric p(CO2). *Geology* 26:143–146. doi: 10.1130/0091-7613(1998)026<0143:VLPART>2.3.CO;2

Elrick, M., Gilleaudeau, G. J., Romaniello, S. J., Algeo, T. J., Morford, J. L., Sabbatino, M., et al. (2022). Major early-middle Devonian oceanic oxygenation linked to early land plant evolution detected using high-resolution U isotopes of marine limestones. *Earth Planetary. Sci. Lett.* 581:117410. doi: 10.1016/j.epsl.2022.117410

Elrick, M., and Witzke, B. (2016). Orbital-scale glacio-eustasy in the middle Devonian detected using oxygen isotopes of conodont apatite: Implications for long-term greenhouse–icehouse climatic transitions. *Palaeogeogr. Palaeoclimatol. Palaeoecol.* 445, 50–59. doi: 10.1016/j.palaeo.2015.12.019

Fehn, U. (2012). Tracing crustal fluids: Applications of natural 129I and 36Cl. *Annu. Rev. Earth Planetary. Sci.* 40, 45–67. doi: 10.1146/annurev-earth-042711-105528

Feng, X., and Redfern, S. A. T. (2018). Iodate in calcite, aragonite and vaterite CaCO3: Insights from first-principles calculations and implications for the I/Ca geochemical proxy. *Geochimica. Cosmochim. Acta* 236, 351–360. doi: 10.1016/j.gca.2018.02.017

Formolo, M. J., Riedinger, N., and Gill, B. C. (2014). Geochemical evidence for euxinia during the late Devonian extinction events in the Michigan basin (U.S.A.). *Palaeogeogr. Palaeoclimatol. Palaeoecol.* 414, 146–154. doi: 10.1016/j.palaeo.2014.08.024

Gensel, P. G., and Andrews, H. N. (1987). The evolution of early land plants. *Am. Scientist.* 75, 478–489. Available at: https://www.jstor.org/stable/27854789

Gilleaudeau, G. J., Algeo, T. J., Lyons, T. W., Bates, S., and Anbar, A. D. (2021). Novel watermass reconstruction in the early Mississippian Appalachian seaway based on integrated proxy records of redox and salinity. *Earth Planetary. Sci. Lett.* 558:116746. doi: 10.1016/j.epsl.2021.116746

Glasspool, I. J., and Scott, A. C. (2010). Phanerozoic concentrations of atmospheric oxygen reconstructed from sedimentary charcoal. *Nat. Geosci.* 3, 627. doi: 10.1038/ngeo923

Hardisty, D. S., Horner, T. J., Evans, N., Moriyasu, R., Babbin, A. R., Wankel, S. D., et al. (2021). Limited iodate reduction in shipboard seawater incubations from the Eastern tropical north pacific oxygen deficient zone. *Earth Planetary. Sci. Lett.* 554:116676. doi: 10.1016/j.epsl.2020.116676

Hardisty, D., Horner, T., Wankel, S., Blusztajn, J., and Nielsen, S. (2020). Experimental observations of marine iodide oxidation using a novel sparge-interface MC-ICP-MS technique. *Chem. Geol.* 532, 119360. doi: 10.1016/j.chemgeo.2019.119360

Hardisty, D. S., Lu, Z., Bekker, A., Diamond, C. W., Gill, B. C., Jiang, G., et al. (2017). Perspectives on proterozoic surface ocean redox from iodine contents in ancient and recent carbonate. *Earth Planetary. Sci. Lett.* 463, 159–170. doi: 10.1016/j.epsl.2017.01.032

Hay, W. W. (1995). Paleoceanography of marine organic-carbon-rich sediments: A. Y. Huc (ed.), Paleogeography, Paleoclimate and Source Rocks, American Association of Petroleum Geologists Memoir 40, 21–59. doi: 10.1306/St40595C2

He, R., Jiang, G., Lu, W., and Lu, Z. (2020a). Iodine records from the ediacaran doushantuo cap carbonates of the Yangtze block, south China. *Precambrian. Res.* 347:105843. doi: 10.1016/j.precamres.2020.105843

He, R., Lu, W., Junium, C. K., Ver Straeten, C. A., and Lu, Z. (2020b). Paleo-redox context of the mid-Devonian Appalachian basin and its relevance to biocrises. *Geochimica. Cosmochim. Acta* 287, 328–340. doi: 10.1016/j.gca.2019.12.019

House, M. R. (2002). Strength, timing, setting and cause of mid-Palaeozoic extinctions. *Palaeogeogr. Palaeoclimatol. Palaeoecol.* 181, 5–25. doi: 10.1016/S0031-0182(01)00471-0

Joachimski, M. M., Breisig, S., Buggisch, W., Talent, J. A., Mawson, R., Gereke, M., et al. (2009). Devonian Climate and reef evolution: Insights from oxygen isotopes in apatite. *Earth Planetary. Sci. Lett.* 284, 599–609. doi: 10.1016/j.epsl.2009.05.028

Johnson, J., Klapper, G., and Elrick, M. (1996). Devonian Transgressive-regressive cycles and biostratigraphy, northern antelope range, Nevada: establishment of reference horizons for global cycles. *Palaios* 11(1):3–14. doi: 10.2307/3515112

Johnson, J., Klapper, G., and Sandberg, C. A. (1985). Devonian Eustatic fluctuations in euramerica. *Geologic. Soc. America Bull.* 96, 567–587. doi: 10.1130/0016-7606(1985)96<567:DEFIE>2.0.CO;2

Johnson, J., and Murphy, M. (1984). Time-rock model for siluro-Devonian continental shelf, western united states. *Geologic. Soc. America Bull.* 95, 1349–1359. doi: 10.1130/0016-7606(1984)95<1349:TMFSCS>2.0.CO;2

Kennedy, H., and Elderfield, H. (1987a). Iodine diagenesis in non-pelagic deep-sea sediments. *Geochimica. Cosmochim. Acta* 51, 2505–2514. doi: 10.1016/0016-7037(87)90301-2

Kennedy, H., and Elderfield, H. (1987b). Iodine diagenesis in pelagic deep-sea sediments. *Geochimica. Cosmochim. Acta* 51, 2489–2504. doi: 10.1016/0016-7037(87)90300-0

Kenrick, P., and Strullu-Derrien, C. (2014). The origin and early evolution of roots. *Plant Physiol.* 166, 570–580. doi: 10.1104/pp.114.244517

Kolata, D. R., and Nelson, W. J. (1990). *Tectonic history of the Illinois basin: Chapter 18: Part i. Illinois basin: Evolution.*

Krause, A. J., Mills, B. J., Zhang, S., Planavsky, N. J., Lenton, T. M., and Poulton, S. W. (2018). Stepwise oxygenation of the Paleozoic atmosphere. *Nat. Commun.* 9, 4081. doi: 10.1038/s41467-018-06383-y

Kump, L. (1988). Terrestrial feedback in atmospheric oxygen regulation by fire and phosphorus. *Nature* 335, 152. doi: 10.1038/335152a0

Küpper, F. C., Feiters, M. C., Olofsson, B., Kaiho, T., Yanagida, S., Zimmermann, M. B., et al. (2011). Commemorating two centuries of iodine research: an interdisciplinary overview of current research. *Angewandte. Chemie. Int. Edition.* 50, 11598–11620. doi: 10.1002/anie.201100028

Lash, G. G., and Blood, D. R. (2014). Organic matter accumulation, redox, and diagenetic history of the Marcellus formation, southwestern Pennsylvania, Appalachian basin. *Mar. Petroleum. Geology.* 57, 244–263. doi: 10.1016/j.marpetgeo.2014.06.001

Lenton, T. M., Dahl, T. W., Daines, S. J., Mills, B. J., Ozaki, K., Saltzman, M. R., et al. (2016). Earliest land plants created modern levels of atmospheric oxygen. *Proc. Natl. Acad. Sci.* 113, 9704–9709. doi: 10.1073/pnas.1604787113

Ling, H.-F., Chen, X., Li, D., Wang, D., Shields-Zhou, G. A., and Zhu, M. (2013). Cerium anomaly variations in ediacaran–earliest Cambrian carbonates from the Yangtze gorges area, south China: Implications for oxygenation of coeval shallow seawater. *Precambrian. Res.* 225, 110–127. doi: 10.1016/j.precamres.2011.10.011

Liu, J., Luo, G., Lu, Z., Lu, W., Qie, W., Zhang, F., et al. (2019). Intensified ocean deoxygenation during the end Devonian mass extinction. *Geochem. Geophys. Geosyst.* 20, 6187–6198. doi: 10.1029/2019GC008614

Lohmann, K. C. (1988). *Geochemical patterns of meteoric diagenetic systems and their application to studies of paleokarst, paleokarst* (Springer), 58–80. Springer, New York, NY.

Lu, W., Dickson, A. J., Thomas, E., Rickaby, R. E. M., Chapman, P., and Lu, Z. (2020a). Refining the planktic foraminiferal I/Ca proxy: Results from the southeast Atlantic ocean. *Geochimica. Cosmochim. Acta* 287, 318–327. doi: 10.1016/j.gca.2019.10.025

Lu, Z., Jenkyns, H. C., and Rickaby, R. E. M. (2010). Iodine to calcium ratios in marine carbonate as a paleo-redox proxy during oceanic anoxic events. *Geology* 38, 1107–1110. doi: 10.1130/G31145.1

Lu, Z., Lu, W., Rickaby, R. E., and Thomas, E. (2020b). Earth History of Oxygen and the iprOxy (Elements in Geochemical Tracers in Earth System Science). Cambridge: Cambridge University Press. doi: 10.1017/9781108688604

Lu, W., Ridgwell, A., Thomas, E., Hardisty, D. S., Luo, G., Algeo, T. J., et al. (2018). Late inception of a resiliently oxygenated upper ocean. *Science* 361, 174–177. doi: 10.1126/science.aar5372

Lu, W., Wörndle, S., Halverson, G., Zhou, X., Bekker, A., Rainbird, R., et al. (2017). Iodine proxy evidence for increased ocean oxygenation during the bitter springs anomaly. *Geochem. Perspect. Lett.* 5, 53–57. doi: 10.7185/geochemlet.1746

Meyer-Berthaud, B., Scheckler, S. E., and Wendt, J. (1999). Archaeopteris is the earliest known modern tree. *Nature* 398, 700–701. doi: 10.1038/19516

Morrow, J. R., and Sandberg, C. A. (2008). Evolution of Devonian carbonate-shelf margin, Nevada. *Geosphere* 4:445–458. doi: 10.1130/GES00134.1

Murphy, A. E., Sageman, B. B., Hollander, D. J., Lyons, T. W., and Brett, C. E. (2000). Black shale deposition and faunal overturn in the Devonian Appalachian basin: Clastic starvation, seasonal water-column mixing, and efficient biolimiting nutrient recycling. *Paleoceanography* 15, 280–291. doi: 10.1029/1999PA000445

Podder, J., Lin, J., Sun, W., Botis, S. M., Tse, J., Chen, N., et al. (2017). Iodate in calcite and vaterite: Insights from synchrotron X-ray absorption spectroscopy and first-principles calculations. *Geochimica. Cosmochim. Acta* 198, 218–228. doi: 10.1016/j.gca.2016.11.032

Pohl, A., Lu, Z., Lu, W., Stockey, R. G., Elrick, M., Li, M., et al. (2021). Vertical decoupling in late Ordovician anoxia due to reorganization of ocean circulation. *Nat. Geosci.* 14, 868–873. doi: 10.1038/s41561-021-00843-9

Rimmer, S. M. (2004). Geochemical paleoredox indicators in Devonian–Mississippian black shales, central Appalachian basin (USA). *Chem. Geology.* 206, 373–391. doi: 10.1016/j.chemgeo.2003.12.029

Sageman, B. B., Murphy, A. E., Werne, J. P., Ver Straeten, C. A., Hollander, D. J., and Lyons, T. W. (2003). A tale of shales: the relative roles of production, decomposition, and dilution in the accumulation of organic-rich strata, middle–upper Devonian, Appalachian basin. *Chem. Geology.* 195, 229–273. doi: 10.1016/S0009-2541(02)00397-2

Shang, M., Tang, D., Shi, X., Zhou, L., Zhou, X., Song, H., et al. (2019). A pulse of oxygen increase in the early mesoproterozoic ocean at ca. 1.57–1.56 Ga. *Earth Planetary. Sci. Lett.* 527, 115797. doi: 10.1016/j.epsl.2019.115797

Stein, W. E., Mannolini, F., Hernick, L. V., Landing, E., and Berry, C. M. (2007). Giant cladoxylopsid trees resolve the enigma of the earth's earliest forest stumps at gilboa. *Nature* 446, 904–907. doi: 10.1038/nature05705

Truesdale, V. W., and Bailey, G. W. (2000). Dissolved iodate and total iodine during an extreme hypoxic event in the southern benguela system. *Estuar. Coast. Shelf. Sci.* 50, 751–760. doi: 10.1006/ecss.2000.0609

van Geldern, R., Joachimski, M. M., Day, J., Jansen, U., Alvarez, F., Yolkin, E. A., et al. (2006). Carbon, oxygen and strontium isotope records of Devonian brachiopod shell calcite. *Palaeogeogr. Palaeoclimatol. Palaeoecol.* 240, 47–67. doi: 10.1016/j.palaeo.2006.03.045

Wallace, M. W., Shuster, A., Greig, A., Planavsky, N. J., and Reed, C. P. (2017). Oxygenation history of the neoproterozoic to early phanerozoic and the rise of land plants. *Earth Planetary. Sci. Lett.* 466, 12–19. doi: 10.1016/j.epsl.2017.02.046

Werne, J. P., Sageman, B. B., Lyons, T. W., and Hollander, D. J. (2002). An integrated assessment of a "type euxinic" deposit: evidence for multiple controls on black shale deposition in the middle Devonian oatka creek formation. *Am. J. Sci.* 302, 110–143. doi: 10.2475/ajs.302.2.110

White, D. A., Elrick, M., Romaniello, S., and Zhang, F. (2018). Global seawater redox trends during the late Devonian mass extinction detected using U isotopes of marine limestones. *Earth Planetary. Sci. Lett.* 503, 68–77. doi: 10.1016/j.epsl.2018.09.020

Wong, G. T., and Brewer, P. G. (1977). The marine chemistry of iodine in anoxic basins. *Geochimica et Cosmochimica Acta.* 41, 151–159. doi: 10.1016/0016-7037(77)90195-8

Zachos, J., Pagani, M., Sloan, L., Thomas, E., and Billups, K. (2001). Trends, rhythms, and aberrations in global climate 65 ma to present. *science* 292, 686–693.doi: 10.1126/science.1059412

Zambito, J. J., Brett, C. E., and Baird, G. C. (2012). The late middle Devonian (Givetian) global taghanic biocrisis in its type area (Northern Appalachian basin): Geologically rapid faunal transitions driven by global and local environmental changes. *Earth Life*, 677–703.doi: 10.1007/978-90-481-3428-1_22

Zhang, F., Dahl, T. W., Lenton, T. M., Luo, G., Shen, S.-Z., Algeo, T. J., et al. (2020). Extensive marine anoxia associated with the late Devonian hangenberg crisis. *Earth Planetary. Sci. Lett.* 533:115976. . doi: 10.1016/j.epsl.2019.115976

Zhou, X., Jenkyns, H. C., Owens, J. D., Junium, C. K., Zheng, X.-Y., Sageman, B. B., et al. (2015). Upper ocean oxygenation dynamics from I/Ca ratios during the cenomanian-turonian OAE 2. *Paleoceanography* 30, 510–526.doi: 10.1002/2014PA002741

Zhou, X., Thomas, E., Rickaby, R. E. M., Winguth, A. M. E., and Lu, Z. (2014). I/Ca evidence for upper ocean deoxygenation during the PETM. *Paleoceanography* 29, 964–975.doi: 10.1002/2014PA002702

Zhou, X., Thomas, E., Winguth, A. M. E., Ridgwell, A., Scher, H., Hoogakker, B. A. A., et al. (2016). Expanded oxygen minimum zones during the late Paleocene-early Eocene: Hints from multiproxy comparison and ocean modeling. *Paleoceanography* 31, 1532–1546. doi: 10.1002/2016PA003020